

NEW CLOSED FORM SOLUTIONS FOR SKELETAL EXTRACTION FROM MOTION CAPTURE

Jonathan Kip Knight
ITT, Colorado Springs, U.S.A.

Sudhanshu Kumar Semwal
Department of Computer Science, University of Colorado, Colorado Springs, U.S.A.

Keywords: Sphere-fit, Motion capture, Skeleton.

Abstract: We present a fast closed form solution for estimating the exact joint locations *inside* the human body from motion capture data. The new closed-form solution is more robust and faster. For example, the formulae are as much as about 100 times faster than the traditional non-linear Maximum Likelihood Estimator and about 9 times faster than linear least squares methods. The methods are proven to be statistically efficient when measurement error is smaller than the joint-marker distance. Unbiased Generalized Delogne-Kása (UGDK), multiple radii solution, and incremental GDK are important contributions of our research providing closed form fast solutions for skeleton extraction from motion capture data. Skeletal animation sequences are generated using the CMU and Eric Camper's motion capture database.

1 INTRODUCTION

Skeleton extraction methods use temporal marker positions from motion capture data to predict the joint locations. These predicted joint locations then define the skeleton. Recently, O'Brien et al., in 2000 (Brian, 2000) and with Kirk (Kirk, 2005) have produced a fast method for skeleton extraction using a linear least squares method assuming there is a relatively stationary point between two segments, and then solving for that point, which is essentially the rotation point. Some years ago, Leendert de Witte (Witte, 1960) found a solution for a circle in 3-D space. The Maximum Likelihood Estimator (MLE) was the first solution for finding the sphere parameters. In 1961 Stephen Robinson (Robinson, 1967) presented the iterative method of solving the sphere and developed a closed form solution for the radius estimator but not for the center estimator. In 1972, Delogne presented (Delogne, 1972) a method for solving a circle for the purposes of determining reflection measurements on transmission lines. István Kása (Kasa, 1976) was the first to recognize the bias in the answer and produced better error analysis. Vaughan Pratt (Pratt, 1987) produced a very generic linear least squares method for

algebraic surfaces. Gander (Gander, 1994) produced the linear least-squares method for circle fitting. Samuel Thomas (Thomas, 1995) created a formula for the Cramér-Rao Lower Bound for the circle estimation. Lukács (Lukas, 1997) produced some improvements on non-linear minimization for spheres. Corral et al. (Corral, 1998) analyzed Kása's formula in more detail and a way to reject the answer if the confinement angle got too small. Strandlie et al. (Strandlie, 2000) transformed a Riemann sphere into a plane and fit the plane using standard methods involving the eigenvalues of the sample covariance matrix. Zelniker (Zelnicar, 2003) reformulated the circle equation to solve directly for the center using the pseudo-inverse ([#]) of a $2 \times N$ matrix. Michael Burr et al. (Burr, 2004) created a geometric inversion technique which far surpassed the complexity needed to solve for a hypersphere. Knight et al. (Knight, 2007) published the initial results from the research for this dissertation in which a skeleton was formed from a closed-form solution of generic motion capture data.

2 SKELETAL EXTRACTION

Producing a skeleton involves finding the centers of joint rotations, the hierarchy of segmentation, and the orientation of each segment. The hierarchy of segmentation is known ahead of time such as in human animation. The orientation of a segment is determined by one of two methods. Either it is given in the raw data, e.g. magnetic trackers, or it is calculated by the fastest technique known. One of the earliest uses found in motion capture were published by Herda et al. (Herada, 2000). The most common approach to calculating a skeleton from motion capture data is through minimization until the skeleton fits where the rotation points have been approximated. The minimization involves squishing segments and moving joints until all joints are nearest to the calculated rotation points. O'Brien et al. (O'Brien, 2000) uses a linear least-squares minimization that produces the rotation points from a collection of time frames. In their study, magnetic motion tracking devices are used which contain both position and orientation. This is akin to solving for the best-fit sphere around a center. 3D marker trajectories are also analyzed in (de-Aguiar, 2006).

In the following section, we start with explanation of symbols and conventions. In Section 4, we visit some methods which have been used in various techniques as a prelude to generalized Generalized Delogne-Kása (GDK) method in Section 5 which include three contributions of our paper – unbiased GDK (Section 6), multiple radii solution (Section 7), and incremental GDK (Section 8). A comparison of all techniques is in Section 10 along with further research (Section 11).



Figure 1: Skeleton from motion capture data.

3 SYMBOLS

- $O(y)$ -- on the order of (i.e. size of) y
- N -- number of measurements
- $CRLB$ -- Cramér-Rao Lower Bound covariance of estimator
- D -- dimension of hypersphere
- $FLOP$ -- floating point operation
- x_i --- i^{th} measurement of position

- \bar{x} --- average of all measurements of positions
- μ_i --- expectation of the i^{th} position
- $\bar{\mu}$ --- average of expectations of all positions
- Σ -- measurement covariance of each position
- $\hat{\Sigma}$ -- measurement covariance estimator
- σ -- measurement standard deviation
- C -- sample covariance
- C_0 -- true covariance of expected positions
- S -- sample third central vector moment
- S_0 -- true third central moment of expected positions
- F_0 -- true 4th central moment of expected positions
- \hat{C} --- center estimator
- C_0 -- true center of hypersphere
- \hat{r} -- radius estimator
- r_0 -- true radius of hypersphere
- λ -- eigenvalue of matrix
- v -- eigenvector of matrix
- x^T -- transpose of column vector into row vector
- A^{-1} -- multiplicative inverse of matrix
- A^T -- transpose of matrix
- ∇ -- vector gradient operator
- $|x|$ -- magnitude of vector
- $|A|$ -- determinant of matrix
- $N_3(\mu, \Sigma)$ -- 3D vector Normal Distribution
- $\rho(A)$ -- spectral radius of matrix
- $Tr(A)$ -- trace (sum of diagonals) of matrix
- $E(A)$ -- expectation of random variate
- $Var(A)$ -- variance of random variate
- $Cov(A, B)$ -- covariance of two variates

4 SPHERICAL CURVE FITTING APPROACHES

There are three techniques in use today: iterative; least squares; and algebraic best fits. They each have their advantages and disadvantages. Iterative techniques are good for accuracy, least squares are faster than iterative but slower than algebraic, and algebraic techniques are good for speed.

4.1 Monte-Carlo Experiments

In order to compare the methods, a Monte-Carlo experiment was run using 1000 trials, each of which had anywhere from 4 to 1,000,000 samples. The runs took over a week of computational effort to collect. Each trial had a fixed standard deviation of the samples from the sphere with values ranging

from 10^{-13} to 10^{14} . The sample must be confined to be within an angle from a fixed point on the sphere. This experiment allows for the in-depth analysis of the error in the answer from four different estimators. The four techniques are Maximum-Likelihood Estimator (MLE) (Section 4.3), Linear Least-Squares (LLS) (Section 4.4), Generalized Delogne-Kása Estimator (GDKE) (Section 5), and the new Unbiased Generalized Delogne-Kása estimator (UGDK) explained in Section 6. The first three are established formulae and has been used for two hundred years (MLE (Shakarji, 1998)) to as young as three years (GDKE (Zelnicker, 2003)). UGDK is new method proposed in this paper. The following graph (Figure 2) shows the errors in the estimators compared to the standard deviation of the samples indicating that UGDK performs closest to CRLB. The graph shows that the relative error versus relative standard deviation is a line for each of these methods. The error is thus proportional to the standard deviation on a log-log display showing a power law. What is also clear from the graph is the comparison. The outliers on the graph have been circled. The obvious differences between the estimators show up in the graph by deviations from the straight line when error equals standard deviation. From the graph, it appears that there is a common limitation to the error in the estimator. This common limitation is named the Cramér-Rao Lower Bound to the covariance of an estimator. The following sections discuss the limit to all estimators for this particular problem. The MLE has outliers when the error equals the radius. This is due to multiple solutions when the error equals the radius. The LLS has outliers when the standard deviation is below about 10^{-6} times the radius and greater than 10^{10} times the radius. These are due to numerical instability during the extremes of using finite representation of decimal numbers. The GDKE seems to be on par with the MLE except for the MLE outliers. The UGDK is consistently close to the CRLB indicating that it is more accurate than other methods.

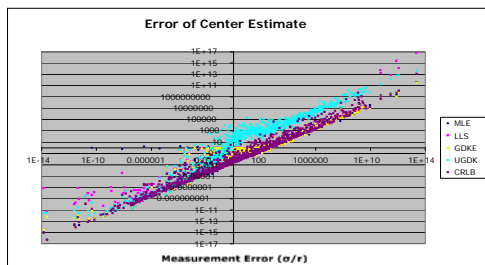


Figure 2: Shows relative error comparison.

4.2 Cramér-Rao Lower Bound (CRLB)

The Cramér-Rao Lower Bound (CRLB) is the proven lower bound for any estimator’s covariance. It is equal to the inverse of the Fisher Information. It is an important measure when dealing with any estimator because it is the best error that an estimator can achieve. All estimators will have at best an error of the CRLB.

4.3 Non-linear Maximum Likelihood Estimator (MLE)

According to the National Institute of Standards and Technology (NIST) (Shakarji, 1998) the best way to find the center of a sphere is through non-linear minimization of the variance of the radius. This is also called the Maximum-Likelihood Estimator (MLE) for the center \hat{c} and radius \hat{r} . The minimization is usually carried out by iterative methods like the Levenberg-Marquardt Method (Shakarji, 1998) and cannot be solved directly.

4.4 Linear Least Square Method (LLS)

The next best thing to the very slow MLE method is through linear least-squares solution. This is usually an over-constrained problem since there are N equations and four (i.e. $D+1$) unknowns. The N equations can be put into a single matrix equation to solve with standard linear algebra techniques. When LLS and CRLB are compared, once again, the outlier cases show that the answer erroneously lies on the sphere. For the most part, the answer error is proportional to the square root of the CRLB. The next fastest algorithm is the linear least squares method which has been analyzed in floating point operations (FLOPs) in (Knight, 2008) with $D=3$ as

$$FLOPs(3) = N236 + 709$$

An estimator of a parameter is considered biased if it is expected to be a little off of the real answer. Zelniker (Zelnicker, 2003) has shown that the bias of the GDKE is on the order of the measurement standard deviation. Our statistical analysis has shown that there are cases when the bias is quite significant and does not disappear even when more samples are taken. The dashed bar in Figure 3 show that the true center is not anywhere within the error ellipsoid of the estimate. This is due solely to the bias in the estimator. This is a good example of why the GDKE has not been adopted as much as the others.

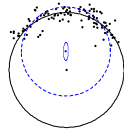


Figure 3: GDKE error ellipse.

5 GENERALIZED DELOGNE-KASA EXPOSITION

The Generalized Delogne-Kása (GDK) estimator (Strandlie, 2000) is the starting basis for our new formulae. This estimator is a general solution for finding the best-fit hypersphere from measurements on the surface. However until now the estimator has limited uses as the estimator is biased and can produce significantly different answers from the solution. The GDK estimator provides a good estimate if the data is evenly distributed over the entire surface of the hypersphere. The estimate falls farther away as the data gets clumped to one side. The GDK estimator is derived from surface measurements x_i and their deviation from a fixed distance from the center. The deviation for N measurements is written as

$$s_{GDK}^2(\hat{c}, \hat{r}) = \frac{1}{N-1} \sum_{i=1}^N \left((x_i - \hat{c})^T (x_i - \hat{c}) - \hat{r}^2 \right)^2 \quad (1)$$

The minimization of this (Knight, 2008) produces estimations for the center and the radius

$$\hat{c} = \bar{x} + \frac{1}{2} \mathbf{C}^{-1} \mathbf{S} \quad (2)$$

$$\hat{r}^2 = \frac{1}{N} \sum_{i=1}^N (x_i - \hat{c})^T (x_i - \hat{c}) \quad (3)$$

where the intermediate quantities include the arithmetic vector mean

$$\bar{x} = \frac{1}{N} \sum_{i=1}^N x_i \quad (4)$$

and the variance-covariance matrix

$$\mathbf{C} = \frac{1}{N-1} \sum_{i=1}^N (x_i - \bar{x})(x_i - \bar{x})^T \quad (5)$$

and the third central vector moment

$$\mathbf{S} = \frac{1}{N-1} \sum_{i=1}^N (x_i - \bar{x})(x_i - \bar{x})^T (x_i - \bar{x}) \quad (6)$$

This estimation of the hypersphere is very fast

due to the Cholesky inverse. The floating point operations for a D -dimensional hypersphere can be counted as

$$FLOPs = N(D^2 + 6D - 1) + \frac{1}{3} D(D+1)(D+8) + 1 \quad (7)$$

which, for the sphere, is

$$FLOPs = N26 + 45 \quad (8)$$

This estimator is about as fast as you can get for this problem but it has one fatal flaw. The estimator has been shown to be biased providing an answer that is offset even under fairly normal conditions. The bias is proportional to the variance of the data (Zelniker, 2004) but analysis here shows the multiplication factor can outweigh an accurate measurement. The bias comes from the fact that one of the variables in the center equation is biased. We consider a measurement system that has a consistent error for each measurement on the surface of the sphere. The measurement is expected to be on the surface but varies from it by the multi-dimensional Gaussian distribution thus

$$x_i = \text{Gaussian}_D(\mu_i, \Sigma) \quad (9)$$

The covariance matrix is then expected to be

$$E(\mathbf{C}) = \mathbf{C}_0 + \Sigma \quad (10)$$

$$\mathbf{C}_0 = \frac{1}{N-1} \sum_{i=1}^N (\mu_i - \bar{\mu})(\mu_i - \bar{\mu})^T \quad (11)$$

$$E(\mathbf{S}) = \mathbf{S}_0 \quad (12)$$

$$\mathbf{S}_0 = \frac{1}{N-1} \sum_{i=1}^N (\mu_i - \bar{\mu})(\mu_i - \bar{\mu})^T (\mu_i - \bar{\mu}) \quad (13)$$

$$E(\hat{c}) = c_0 + \frac{1}{2} \left((\mathbf{C}_0 + \Sigma)^{-1} - \mathbf{C}_0^{-1} \right) \mathbf{S}_0 + \dots \quad (14)$$

6 UNBIASED GDK

Unbiased GDK provides a quick method to draw a skeleton from motion capture data. The main contribution to the state of the art is that the estimator explained below is asymptotically unbiased. Asymptotically unbiased is defined as an inversely proportional relationship with the sample count: $E(\hat{q}) = q_0 + O(\frac{1}{N})$ where q_0 is the parameter that the estimator is trying to estimate. This basically says that the estimator is expected to get closer to the true answer if more samples are taken. It is shown in (Knight, 2008) that the GDKE estimators for center and radius do not satisfy this requirement.

Our algorithm uses a simple substitution that turns the GDKE into one with a diminishing bias. It involves the use of an a-priori estimate of the measurement error in the samples. This is very reasonable since most systems of measurement have some kind of estimate to the measurement error. Since the sample covariance matrix \mathbf{C} is the only biased term in the equation for the GDKE center, this is what will be altered.

$$\mathbf{C}' = \mathbf{C} - \hat{\Sigma} \quad (15)$$

$$E(\mathbf{C} - \hat{\Sigma}) = \mathbf{C}_0 + \Sigma - \hat{\Sigma} \quad (16)$$

$$\hat{c}_u = \bar{x} + \frac{1}{2}(\mathbf{C} - \hat{\Sigma})^{-1} \mathbf{S} \quad (17)$$

$$\hat{r}_u = \sqrt{\frac{N-1}{N} \text{Tr}(\mathbf{C} - \hat{\Sigma}) + (\bar{x} - \hat{c}_u)^T (\bar{x} - \hat{c}_u)} \quad (18)$$

$$\text{Tr}(\hat{\Sigma}) = \frac{1}{N} \sum_{i=1}^N (x_i - c_0)^T (x_i - c_0) - r_0^2 \quad (19)$$

This leads to fastest, asymptotically unbiased estimator of a hypersphere in (Knight, 2008) as

$$\hat{c}' = \bar{x} + \frac{1}{2}(\mathbf{C} - \hat{\Sigma})^{-1} \mathbf{S} \quad (20)$$

$$\hat{r}' = \sqrt{\frac{N-1}{N} \text{Tr}(\mathbf{C} - \hat{\Sigma}) + (\bar{x} - \hat{c}')^T (\bar{x} - \hat{c}')} \quad (21)$$

A typical use of these new estimators can be displayed using Mathematica, with exactly the same data as used for displayed for the GDKE. The true center is within the error ellipsoid (Figure 4). This data contains 100 points generated with a diagonal measurement covariance with all diagonals equal to 0.05^2 . The Leontief condition ($\rho < 1$) is satisfied with the spectral radius in question equal to 0.557238. These equations show that there still is a bias, but it is asymptotically unbiased. We implemented (results in Figure 4). A Monte-Carlo run that explicitly shows the $1/\sqrt{N}$ dependency. The error in the estimate is compared with how many points were analyzed for a particular joint in given motion capture data.

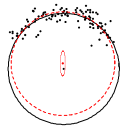


Figure 4: UGDK error ellipse.

An example analysis using MLE, UGDK and GDKE is presented in Figure 5. The figure clearly shows the improvement over the GDKE with same FLOP count for UGDK as GDKE. The figure shows

the bias is removed using the UGDK and results produced by UGDK are close to MLE. The FLOP counts for UGDK remains same as GDK (Knight 2008). Our analysis in (Knight 2008) also shows that there is a case when all methods have troubles in estimating the joint location – this is the case when measurement error is actually bigger than the item being measured. This situation is a bit impractical, as no one wants such a system of measurement.

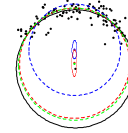


Figure 5: Comparison of methods.

7 NEW SOLUTION: MULTIPLE RADII SOLUTION

For multiple markers going around the same center of rotation, another formula can be achieved by the same analysis of least squares. This technique is good to use when more than one marker is available. It has the ability to average out errors when one marker is too close to the rotation point or has other systematic problems. Excluding the derivation, we have the following equations for center and radius estimates where M is the number of markers and subscript p indicates values that utilize the single marker's positions:

$$\hat{c}_m = \left(\sum_{p=1}^M (\mathbf{C}_p - \hat{\Sigma}) \right)^{-1} \sum_{p=1}^M (\mathbf{C}_p - \hat{\Sigma}) \bar{x}_p + \frac{1}{2} \mathbf{S}_p \quad (22)$$

$$\hat{r}_p = \sqrt{\frac{N-1}{N} \text{Tr}(\mathbf{C}_p - \hat{\Sigma}) + (\bar{x}_p - \hat{c}_m)^T (\bar{x}_p - \hat{c}_m)} \quad (23)$$

Symbols and conventions are given in Section 2.

The matrix that is to be inverted here is still a positive-definite matrix since positive-definite matrices added together still produce a positive-definite matrix. This allows for the speedier Cholesky decomposition and the singular values can be excluded. An example of the MGDK method is presented in Figure 6. This example shows what happens when the individual circles are compared to that when combined in the MGDK. The outer circle solution is drawn in red; the inner circle solution is drawn in blue, and the MGDK solution is drawn in green. The example shows a dramatic improvement over both of the individual circle calculations. FLOP count analysis is in (Knight, 2008).

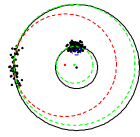


Figure 6: Comparison of methods.

8 NEW SOLUTION: IGDK

A more refined answer can be achieved when using an incremental improvement GDK (IGDK) formula. The idea here is a group of samples are collected and an answer is retrieved from the GDKE or UGDK formulae. Excluding the derivation, we have the following equations. Equations for S and C for (n+1)th sample are defined in (Knight, 2008) and are calculated using recurrence relationship. Below are the final equations for the center and radius. The advantage is that no new matrix inverse is needed and the storage requirements are of constant order.

$$\hat{c}_{n+1} = \bar{x}_{n+1} + \frac{1}{2} \mathbf{C}_{n+1}^{-1} \mathbf{S}_{n+1} \quad (24)$$

$$\hat{r}_{n+1}^2 = \frac{n}{n+1} \text{Tr}(\mathbf{C}_{n+1}) + (\bar{x}_{n+1} - \hat{c}_{n+1})^T (\bar{x}_{n+1} - \hat{c}_{n+1}) \quad (25)$$

When compared to the FLOPs for the GDKE method, this incremental approach is about four times slower. This makes the incremental approach a last resort when a few extra points need to be added to a previously calculated center and radius. This new estimator has the distinct advantage of constant memory requirements no matter how many points are analyzed.

9 EXPERIMENTS

9.1 Case Study – CMU Data

The CMU Graphics Lab produced a one minute long motion capture data-set of a salsa dance in 60-08. The data file contains 3421 time slices for 41 markers on two figures. This case study will concentrate on analyzing the performance of the UGDK in determining the rotation points in the female subject. Four data sets were created by removing random samples from the CMU data sets. 400 rotation points were collected. The calculated constants are the relative rotation points as referenced in each segment's parent's coordinate system. The 400 calculations were averaged and the standard deviations were calculated as well. Details results are analyzed in (Knight, 2008) Most of the

standard deviations are less than one centimeter, but there are some significant outliers like the right ankle. Further analysis of the calculated points for the ankles and elbows shows that the four runs produced two answers due to different orientations of the parent's reference frame. As can be readily seen from the above graph, a statistically significant amount of calculations are within one centimeter of accuracy when analyzing more than about 200 samples. The accuracy gets better on average with a power law close to $1/\sqrt{N}$ (Figure 7). Skeletal animation of our results is provided in mpeg files.

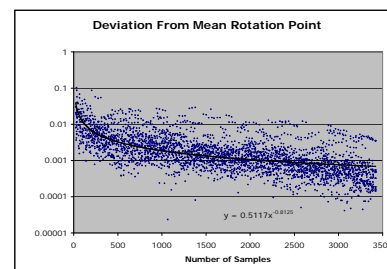


Figure 7: Inverse Power Law.

9.2 Case Study of Eric Camper's ACCAD Data

The motion capture data in the ericcamper.c3d (Motion was analyzed to produce a skeleton. The subject did various martial arts maneuvers that moved every joint involved in drawing. One time frame is presented in the following figure. We show a frame of animation in Figure 1 which shows what appears to be a natural pose for all joints during a karate exercise.

10 RESULTS

A Monte-Carlo experiment was set up to determine the speed of the various sphere-fit algorithms. Up to a million samples were chosen on a sphere with varying measurement error, confinement angle, sphere-center and sphere-radius. The measurement error varied from 1×10^{-11} to 1×10^{12} . The confinement angle varied from 0 to 180° . The sphere center varied as much as 2 around the origin. The radius varied 0 to 37. The linear algebra algorithms were all implemented from well-accepted implementations presented in Numerical Recipes in C (Press, 1992) The code was compiled optimized for a PowerPC G4 processor and run on a 1GHz Apple PowerBook 12".

As discussed in (Knight, 2008), the GDKE, and therefore UGDK, is always faster with FLOP count as $26N$. The GDKE/UGDK is 2.17 times faster than IGDK on average. Based on FLOP counts as explained in (Knight, 2008) in detail, the GDKE/UGDK is 11.05 times faster than the LLS method and about 80 times faster than the MLE when the measurement error is less than one.

10.1 Summary of Important Results

Three new closed-form methods have been presented to find rotation points of a skeleton from motion capture data. A generic skeleton can be directly extracted from noisy data with no previous knowledge of skeleton measurements. The new methods are ten times faster than the next fastest and a hundred times faster than the most widely accepted method. Two phases are used to produce an accurate skeleton of the captured data. The *first phase*, fitting the skeleton, is robust even with noisy motion capture data. As explained earlier, the formulae use an asymptotically unbiased version of the Generalized Delogne-Kása (GDKE) Hyperspherical Estimation (i.e UGDK). The second estimator takes advantage of multiple markers located at different distances from the rotation point (MGDK) thereby increasing accuracy. The third estimator incrementally improves an answer and has advantages of constant memory requirements suitable for firmware applications (IGDK). The UGDK produces the answer faster than any previous algorithm and with the same efficiency with respect to the Cramér-Rao Lower Bound for fitting spheres and circles. The UGDK method significantly reduces the amount of work needed for calculating rotation points by only requiring $26N$ flops for each joint. The next fastest method, Linear Least-Squares requires $236N$ flops. In-depth statistical analysis shows the UGDK method converges to the actual rotation point with an error of $O(\sigma/\sqrt{N})$ improving on the GDKE's biased answer of $O(\sigma)$. The *second phase* is a real-time algorithm to draw the skeleton at each time frame with as little as one point on a segment. This speedy method, on the order of the number of segments, aids the realism of motion data animation by allowing for the subtle nuances of each time frame to be displayed. Flexibility of motion is displayed in detail as the figure follows the captured motion more closely. With the reduced time complexity, multiple figures, even crowds can be animated. In addition, calculations can be reused for the same actor and marker-set allowing different data sets to be blended.

11 CONCLUSIONS

In our effort to try to speed up skeleton extraction from motion capture data we discovered a new asymptotically unbiased GDK (UGDK) formulation which fills the vital low-level hole and makes GDK formulation practical. This paper presents the fastest known general method for calculating the rotation points and can be as much as ten times faster than the next fastest method available as explained in (Knight, 2009) The UGDK method has further impact in a vast collection of fields as diverse as character recognition to nuclear physics where an algorithm is needed for the speedy recovery of the center of a circle or sphere. The UGDK is expected to play a vital role in the process of determining a skeleton from motion capture data. The MGDK adds robustness to the equations allowing to use every bit of available data. The IGDK further has the application of being an ideal algorithm to burn into a silicon chip whose memory requirements are constrained.

The UGDK estimators are an improvement on existing science but they are strictly dependent on a-priori knowledge of the measurement error. It has been shown that the measurement error trace can itself be estimated but not the whole measurement covariance matrix. An estimator for the whole matrix would be most ideal but was not found in the course of this study and should be a topic of future research. The main contributions are the new unbiased center formulae; the full statistical analysis of this new formula; and the analysis of when the best measurement conditions are to initiate the formula. The research further establishes the application of these new formulae to motion capture to produce a real-time method of drawing skeletons of arbitrary articulated figures. is advisable to keep all the given values.

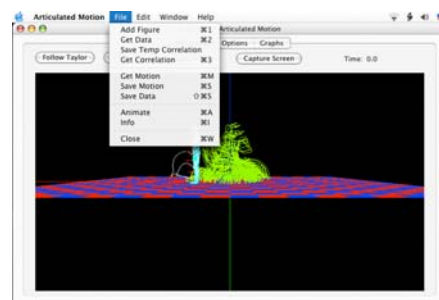


Figure 8: A sample of File menu interface.

ACKNOWLEDGEMENTS

We wish to thank all the reviewers of the paper, especially numbers 3 and 4, for their insightful comments.

REFERENCES

- Aguiar, D., Theobalt, C., Seidal, H., Automatic learning of articulated Skeletons from 3D marker Trajectories, in *International Symposium, ISVC 2006*, part I, Springer-Verlag, Lecture Notes in Computer Science, vol. 4291, pp. 485-494 (2006).
- O'Brien, J. F., Bodenheimer Jr R. E. , Brostow G. J., and Hodgins J. K.. *Automatic Joint Parameter Estimation from Magnetic Motion Capture Data*, pages 53–60, Montreal, Quebec, Canada, May 15-17 2000. Graphics Interface.
- Burr, M., Cheng, A., Coleman, R., and Souvaine, D., Transformations and Algorithms for Least Sum of Squares Hypersphere Fitting. *16th Canadian Conference on Computational Geometry*, 2004, pp 104-107.
- Camper, E., Motion Capture Data accacad.osu.edu/research/mocap/mocap_research.html
- Corral, C., Lindquist, C., On implementing Kása's circle fit procedure. *IEEE Transactions on Instrumentation and Measurement*, 47(3):789–795, June 1998.
- Delogne, P., Computer Optimization of Deschamps Method and Error Cancellation in Reflectometry. In *Proceedings of the IMEKO Symposium on Microwave Measurements, Budapest, Hungary*, May 1972, pp. 117-129.
- Gander, W., Golub, G., Strelbel, R., Least-Squares Fitting of Circles and Ellipses. *BIT Numerical Mathematics* 34, Springer 1994, pp 558-578.
- Herda, L., Fua, P., Plankers, R., Boulic, R., D. Thalmann, D., Skeleton-based motion capture for robust reconstruction of Human Motion, *Computer Animation* (book), Philadelphia, PA, pp.77-May (2000).
- Kása, I., A circle fitting procedure and its error analysis. *IEEE Transactions on Instrumentation and Measurement*, 25:8–14, March 1976.
- Kirk, A. G., O'Brien, J., Forsyth, D.A. Skeletal parameter estimation from optical motion capture data. In *IEEE Conf. on Computer Vision and Pattern Recognition (CVPR)*. IEEE, 2005.
- Knight, J., Semwal, S., Fast Skeleton estimation from motion captured using Generalized Delogne-Kasa method, In *15th International Conference in Central Europe on Computer Graphics, Visualization and Computer Vision, Plzen, WSCG Conference Proceedings*, pp. 225-232, ISBN 978-80-86943-98-5, Feb 2007.
- Knight, J., Rotation Points from Motion Capture Data using a closed form solution, *PhD thesis*, University of Colorado at Colorado Springs, Advisor Professor Semwal, SK., pp. 1-152 (2008).
- Lukács, G., Marshall, A., Martin, R., Geometric Least-Squares Fitting of Spheres, Cylinders, Cones, and Tori *RECCAD Deliverable Documents 2 and 3 Copernicus Project No. 1068* Reports on basic geometry and geometric model creation, etc. Edited by Dr. R. R. Martin and Dr. T. Varady Report GML 1997/5, Computer and Automation Institute, Hungarian Academy of Sciences, Budapest, 1997.
- Pratt, V., Direct least-squares fitting of algebraic surfaces. *Computer Graphics*, 21(4):145–152, July 1987.
- Press, W., Teukolsky, T., Vetterling, W., Flannery, B., *Numerical Recipes in C: The Art of Scientific Computing*. 2nd.ed., Cambridge University Press: 1992.
- Robinson, S. Fitting Spheres by the Method of Least Squares, In *Communications of the ACM*, Volume 4, No. 11; November 1967, p. 491.
- Shakarji, C., Least-Squares Fitting Algorithms of the NIST Algorithm Testing System, *J. of Research of the National Institute of Standards and Technology*: 103, No. 6 (1998): 633.
- Strandlie, A., Wroldsen, J., Frühwirth, R., and Lillekjendlie, B., Track Fitting on the Riemann Sphere. *International Conference on Computing in High Energy and Nuclear Physics*, Padova, Italy; February, 2000.
- Thomas S., Chan, Y., Cramer-Rao Lower Bounds for Estimation of a Circular Arc Center and Its' Radius. *CVGIP: Graphics Model and Image Processing*, Vol. 57, No. 6, pages 527-532, 1995.
- Witte, L., Least Squares Fitting of a Great Circle Through Points on a Sphere. *Communications of the ACM*, Volume 3, No. 11, November 1960, pp. 611-613.
- Zelniker E., Clarkson, I., A Statistical Analysis Least-Squares Circle-Centre Estimation. In *IEEE International Symposium on Signal Processing and Information Technology*, December 2003, Darmstadt, Germany, pp 114-117.
- Zelniker, E., Clarkson, I., A Generalisation of the Delogne-Kása Method for Fitting Hyperspheres. *Thirty-Eighth Asiomar Conference on Signals, Systems and Computers*. Pacific Grove, California, November 2004.